A Complex-Analytic Formulation of Black Hole Thermodynamics

Wen-Xiang Chen*

School of Electronic Information, Guangzhou City University of Technology, Guangzhou 510800, China

Yao-Guang Zheng†

Department of Physics, College of Sciences, Northeastern University, Shenyang 110819, China

Abstract

The pole of the radial optical one-form fixes the Hawking temperature of a static, non-degenerate horizon. We ask how much of the thermodynamic metric can be recovered by following its residue b along a family of black holes with a common normalization of Killing time. With the entropy S specified, the fixed-charge heat capacity obeys $C^{-1} = -\partial_S \log b$. Knowing b throughout the state space fixes the entropy row of the metric but leaves an arbitrary function of charge in the thermodynamic potential. Two locally stable potentials with the same temperature field can consequently have different scalar curvatures. Four-dimensional charged anti-de Sitter black holes illustrate why the distinction matters. At the canonical critical pressure P_c, the heat capacity has a double pole in the horizon radius and the ordinary two-variable curvature stays finite. At $3P_c$, a fixed-charge curve meets the metric-degeneracy locus tangentially. Along that curve the curvature has a fourth-order pole and the heat capacity stays finite. Continuing the temperature derivative into the complex radius plane explains how its two real zeros leave the physical branch while their total contour index is conserved. Equality of the free energies at two distinct radii supplies the separate condition for phase coexistence.

Keywords black hole thermodynamics, thermodynamic geometry, horizon residue, analytic continuation, heat capacity, charged AdS black holes

1 Introduction

For an asymptotically flat charged black hole, the fixed-charge heat capacity diverges at $r_+^2 = 3Q^2$, yet the two-variable entropy metric is flat across that radius. There are two derivatives at issue. The radial derivative of the metric in one spacetime fixes its Hawking temperature. A temperature derivative along a family of equilibrium spacetimes fixes the response to a change in mass. The optical residue makes it possible to carry the first calculation into the second without identifying the two radial variables.

The four laws of black-hole mechanics, the area dependence of entropy, and Hawking's particle-creation calculation fix the physical normalization of the temperature and entropy used here [1–3]. Analyticity enters both the propagator derivation and the Euclidean periodicity argument [4,5]. It also governs the choice of path across the horizon in tunneling calculations [6–8]. Robson, Villari and Biancalana (RVB) recovered the temperature from the topology of the two-dimensional Euclidean section [9]. A Laurent expansion at the horizon recasts this calculation in terms of a local contour integral [10, 13]. Related calculations cover charged and rotating solutions in modified gravity [11, 12]. In a quadratic-gravity background the same coefficient multiplies the logarithm in the scalar tortoise coordinate [13]. Recovering entropy requires further input

*Email: chenwx@gcu.edu.cn

†Email: hesoyam12456@163.com

through a first law or a normalized Noether charge [14,15]. Here the question is what the residue determines once the entropy coordinate has been supplied.

Weinhold and Ruppeiner define their metrics by differentiating a thermodynamic potential twice in preferred coordinates [16–18]. For Reissner–Nordström (RN) black holes, the ordinary entropy metric distinguishes the asymptotically flat family from the anti-de Sitter (AdS) family, whose curvature can diverge [19]. Davies studied singular heat capacities in the charged and rotating problem [20]. Whether a curvature singularity detects such a divergence depends on the potential [21–23] and on the state variables allowed to fluctuate [24,25]. A Legendre-invariant metric is another available choice [26]. The choice also enters geometric studies of charged solutions in modified gravity [27]. We work at fixed pressure, take the entropy Hessian in (M, Q), and transform it as a tensor to (S, Q). This specifies the curvature used in the flat RN example above.

Complex classifications of black-hole phases have used defects of an off-shell free energy [28], the residues associated with their winding [29], and the zeros of analytically continued free-energy derivatives [30–32]. The number of real temperature extrema has also been related to equilibrium branch counts and complex foliations [33]. Xu and Mann obtained the charged-AdS spinodal polynomial and traced its roots into the complex plane [34]. We compare that polynomial with the determinant of the thermodynamic metric and obtain two different pole collisions on the same black-hole family, Eqs. (3.18) and (3.19). A separate inverse calculation in Sec. 4 identifies the charge response that a horizon-temperature measurement leaves undetermined.

2 From the optical pole to a derivative on state space

2.1 Euclidean normalization of the residue

Work in units $G = \hbar = c = k_{\mathrm{B}} = 1$. First fix one black hole and its Killing time t. Its static, spherically symmetric exterior has line element

$$ds^2 = -A(w)\,dt^2 + \frac{dw^2}{B(w)} + w^2 d\Omega_2^2. \tag{2.1}$$

Here w is the areal radius. To continue it into the complex plane, assume that A and B are real analytic and have simple zeros at the outer horizon $w = h$, with positive derivatives a_1, b_1. Write $\xi = w - h$. Within their common disk of convergence, $A = a_1\xi + a_2\xi^2 + O(\xi^3)$ and $B = b_1\xi + b_2\xi^2 + O(\xi^3)$. Factoring $a_1 b_1 \xi^2$ from the product gives the analytic square root

$$\sqrt{AB} = \sqrt{a_1 b_1}\,\xi\left[1 + \frac{1}{2}\left(\frac{a_2}{a_1} + \frac{b_2}{b_1}\right)\xi + O(\xi^2)\right]. \tag{2.2}$$

Its sign agrees with the positive square root in the real exterior $\xi > 0$. A radial null ray satisfies $dt = \pm dw/\sqrt{AB}$. Expanding this optical one-form ω gives

$$\omega = \frac{dw}{\sqrt{AB}} = b\left[\frac{1}{\xi} - \frac{1}{2}\left(\frac{a_2}{a_1} + \frac{b_2}{b_1}\right) + O(\xi)\right]d\xi, \tag{2.3}$$

$$b = \operatorname*{Res}_{w=h}\omega = \frac{1}{2\pi i}\oint_{\gamma_h}\omega = \frac{1}{\sqrt{a_1 b_1}}. \tag{2.4}$$

Integrate on a positively oriented loop γ_h enclosing only the horizon. A primitive of ω contains $b\log\xi$, so one turn adds $2\pi i b$. For comparison, $d\log A$ has residue 1 because $A = \xi(a_1 + O(\xi))$. The Schwarzschild function in Eq. (4.6) of Ref. [10] illustrates the distinction. At $w = 2M$ the metric function has a simple *zero*, and its reciprocal times dw has a pole. The former has integer multiplicity while the latter has a residue b with units of length.

To find the thermal period, set $t = -i\tau$ and $\rho = 2\sqrt{\xi/b_1}$. Substituting $\xi = b_1\rho^2/4$ and $d\xi = (b_1\rho/2)d\rho$ gives $d\xi^2/B = [1 + O(\rho^2)]d\rho^2$ and $A\,d\tau^2 = (a_1 b_1/4)\rho^2[1 + O(\rho^2)]d\tau^2$. The angle

at the Euclidean origin is therefore $\sqrt{a_1 b_1}\,\tau/2$. Requiring this angle to have period 2π fixes the period of the chosen time coordinate,

$$\kappa = \tfrac{1}{2}\sqrt{a_1 b_1}, \qquad \beta = \frac{2\pi}{\kappa} = 4\pi b, \qquad T_H = \frac{1}{4\pi b}. \tag{2.5}$$

The thermal period is twice the magnitude of the optical monodromy on the real exterior branch [5, 15]. For Schwarzschild, $A = B = 1 - 2M/w$ gives $\omega = (1 + 2M/(w - 2M))dw$, so $b = 2M$ and $T_H = 1/(8\pi M)$.

In Schwarzschild gauge $A = B = f$, the two-dimensional topological construction gives the same period [9]. Cut off the Euclidean orbit-space disk at $w = L > h$. The two-dimensional metric has unit determinant, and its Christoffel symbols $\Gamma^w_{\tau\tau} = -ff'/2$, $\Gamma^\tau_{w\tau} = f'/(2f)$, and $\Gamma^w_{ww} = -f'/(2f)$ give $R^{(2)} = -f''$. At the outer circle the line element is $ds = \sqrt{f(L)}d\tau$. With the boundary orientation of the disk, its geodesic curvature contributes $k_g\, ds = f'(L)d\tau/2$. Gauss–Bonnet then gives

$$1 = \frac{\beta}{4\pi}\int_h^L [-f''(w)]\, dw + \frac{\beta}{4\pi} f'(L) = \frac{\beta f'(h)}{4\pi}. \tag{2.6}$$

The boundary term cancels the contribution at L, leaving only the horizon slope $f'(h) = 1/b$. This disk argument requires a common smooth Euclidean period. Horizons with incompatible periods violate that requirement.

2.2 Varying the solution while keeping the clock fixed

Now compare neighboring black holes. The state parameter z labels the solution, while w remains the radial coordinate within each solution. Let the family be holomorphic at fixed work variables, with a simple horizon $h(z)$. Choose the same normalization of Killing time throughout and use the branch with $T > 0$ on the real slice. For z sufficiently close to its base value, one fixed circle in the w-plane encloses the moving horizon and no other pole. Factoring the optical denominator as $(w - h(z))\, U(w, z)$, with U holomorphic and nonzero, gives

$$b(z) = \frac{1}{2\pi i}\oint_\gamma \omega(w; z) = \frac{1}{U(h(z), z)}, \qquad b'(z) = -\frac{U_w(h, z)h'(z) + U_z(h, z)}{U(h, z)^2}. \tag{2.7}$$

Both terms in $b'(z)$ matter. One accounts for the motion of the horizon, the other for the explicit dependence of the metric on the state. In logarithmic derivatives, $\log b$ denotes $\log(b/b_{\mathrm{ref}})$ for any fixed nonzero reference length. Substitution in the contour integral shows that a holomorphic radial change of coordinates with nonzero Jacobian preserves b. A common rescaling of the Killing time multiplies b by a constant and hence preserves $d\log b$. A rescaling that varies from state to state contributes its own logarithmic derivative. Equation (2.7) continues the branch chosen at the real base point. Replacing this continuation by its modulus would lose holomorphicity.

To pass from temperature to entropy, assume a thermodynamic mass and an independently normalized entropy satisfying $dM = T\, dS$ at fixed work variables, with $T = T_H$. Integrating on a simply connected regular patch using Eq. (2.5) gives

$$S(z) - S(z_0) = 4\pi \int_{z_0}^{z} b(\zeta) M'(\zeta)\, d\zeta. \tag{2.8}$$

The integrand requires the variation of mass across the family, and the additive constant requires an entropy reference [14]. When the work variables vary too, the corresponding one-form is $T^{-1}(dM - \Phi\, dQ - V\, dP)$. Closure ensures a local entropy function. A global single-valued entropy also requires vanishing periods around noncontractible cycles. The Einstein action fixes the area normalization, while higher-curvature theories require the corresponding charge prescription [35, 36]. An integer contour count contains no such normalization.

On a fixed-control curve, suppose $S'(z) \neq 0$. Differentiating $4\pi bT = 1$ along this curve and using $dT/dS = T'/S'$ in the definition of the heat capacity gives

$$\frac{T'}{T} = -\frac{b'}{b}, \qquad \frac{1}{C} = \frac{1}{T}\frac{T'}{S'} = -\frac{b'}{bS'}, \qquad C = -\frac{bS'}{b'}. \tag{2.9}$$

The identities extend meromorphically wherever the state functions do, provided T' is not identically zero. In particular, $1/C$ extends through an isolated zero of b'. For the Schwarzschild family choose $z = 2M$. Then $S = \pi z^2$, $b = z$, and Eq. (2.9) gives $C = -2\pi z^2 = -8\pi M^2$, while Eq. (2.8) gives $dS = 2\pi z\, dz$. This negative heat capacity refers to an unconfined black hole. A finite thermal cavity changes the temperature at the boundary and the resulting stability criterion [37].

2.3 Why the simple-horizon hypothesis matters

For asymptotically flat RN, $f(w) = (w - r_+)(w - r_-)/w^2$ with $r_\pm = M \pm \sqrt{M^2 - Q^2}$. For distinct horizons $r_+ > r_-$, partial fractions give the two optical residues

$$b_+ = \frac{r_+^2}{r_+ - r_-}, \qquad b_- = -\frac{r_-^2}{r_+ - r_-}, \qquad b_+ + b_- = r_+ + r_-. \tag{2.10}$$

As $r_\pm \to r_e = |Q| > 0$, $b_+ \to +\infty$ and $T_H \to 0$. At the coincident root the one-form instead has Laurent expansion

$$\omega = \left[\frac{r_e^2}{(w - r_e)^2} + \frac{2r_e}{w - r_e} + 1\right] dw. \tag{2.11}$$

The residue $2r_e$ is the limit of the sum measured by a contour that encloses both poles. A contour isolating the outer pole before the merger measures b_+, which diverges. The proper radial distance of the extremal solution contains $\int dw/(w - r_e)$ and diverges logarithmically. The Euclidean section therefore loses the finite-distance polar origin that fixed the temperature in the simple-horizon case [15, 38].

3 Complex continuation of the thermodynamic metric

3.1 Choice of thermodynamic coordinates

Let $M(S, Q)$ be real analytic on an open set of equilibrium states, with all external parameters held fixed. For an AdS black hole at fixed pressure, M is the enthalpy. In the thermodynamic coordinates $x = (S, Q)$ the first derivatives are $T = M_S$ and $\Phi = M_Q$. One can take the Hessian of M in these coordinates or the negative Hessian of the entropy in $y = (M, Q)$,

$$W_{ij} = \frac{\partial^2 M}{\partial x^i \partial x^j}, \qquad g^{(y)}_{ab} = -\frac{\partial^2 S}{\partial y^a \partial y^b}. \tag{3.1}$$

Each definition singles out the coordinates of its own thermodynamic representation [16–19]. A fluctuation interpretation requires the quadratic form to be positive on the real fluctuations allowed by the ensemble.

Where $T \neq 0$, the inverse function theorem allows us to solve $M(S, Q)$ locally for $S(M, Q)$. The first law then gives $S_{,M} = 1/T$ and $S_{,Q}|_M = -\Phi/T$. The composition $S(y(x)) = x^1$ is linear in x. Taking its second derivatives gives

$$0 = S_{,ab} y^a{}_{,i} y^b{}_{,j} + S_{,a} y^a{}_{,ij} = S_{,ab} y^a{}_{,i} y^b{}_{,j} + \frac{1}{T} M_{,ij}. \tag{3.2}$$

The Q component of $y(x)$ contributes no second derivatives because it is linear. Thus the entropy-Hessian metric in the (S, Q) chart is

$$g_{ij} = g^{(y)}_{ab} y^a{}_{,i} y^b{}_{,j} = \frac{W_{ij}}{T}. \tag{3.3}$$

Once g has been defined in a thermodynamic chart, it transforms by tensorial pullback. Recomputing the ordinary Hessian of M after a nonlinear coordinate change would add the chain-rule term $M_{,i}\,\partial_\alpha\partial_\beta x^i$.

At an interior point, the Taylor series of M converges on a sufficiently small complex polydisc and defines a holomorphic germ $\mathcal{M}(z^1, z^2)$. Its coefficients are fixed by the derivatives on the real state space, so the extension is unique as a germ. On this polydisc set

$$\mathcal{T} = \partial_1\mathcal{M}, \qquad \mathcal{W}_{ij} = \partial_i\partial_j\mathcal{M}, \qquad \}_{ij} = \frac{\mathcal{W}_{ij}}{\mathcal{T}}. \tag{3.4}$$

The resulting symmetric complex-bilinear form is holomorphic and nondegenerate where $\mathcal{T}\det\mathcal{W} \neq 0$. Indeed, $\det\} = \det\mathcal{W}/\mathcal{T}^2$ and $\}^{-1} = \mathcal{T}\,\mathrm{adj}(\mathcal{W})/\det\mathcal{W}$. The connection and curvature are holomorphic on this regular set. They extend meromorphically to the polydisc provided neither denominator vanishes identically. A zero in a denominator gives only a candidate pole until common factors have been cancelled. A square-root coordinate requires a choice of branch on which the coordinate change is locally biholomorphic. Positivity enters only on the real state space.

The heat capacity samples a single direction in the state space. At fixed Q and $T \neq 0$ its denominator can be compared directly with the determinant of the full Hessian,

$$C_Q = T\left(\frac{\partial S}{\partial T}\right)_Q = \frac{T}{M_{SS}}, \qquad \det W = M_{SS}M_{QQ} - M_{SQ}^2. \tag{3.5}$$

At $M_{SS} = 0$ with $M_{SQ} \neq 0$, $\det W = -M_{SQ}^2 \neq 0$. The fixed-charge heat capacity can thus diverge where the full metric is regular. On the real slice its Hessian has negative determinant at this point and therefore has indefinite signature. Allowing charge to fluctuate changes the stability question.

3.2 The charged Einstein–Maxwell family at fixed pressure

For a four-dimensional charged black hole, both singularity tests can be evaluated in terms of the outer horizon radius r, used here as a coordinate on the family of equilibrium states. Set $a = 8\pi P = 3/\ell^2$ for AdS and $a = 0$ for asymptotic flatness. The horizon equation for the metric function $1 - 2M/r + Q^2/r^2 + ar^2/3$ and the area entropy give

$$M = \frac{r}{2} + \frac{Q^2}{2r} + \frac{ar^3}{6}, \qquad S = \pi r^2, \qquad \partial_S|_Q = \frac{1}{2\pi r}\,\partial_r|_Q\,. \tag{3.6}$$

Choose the branch $r = \sqrt{S/\pi}$ that is positive at the real base point. Introduce $u = Q/r$ and three dimensionless functions,

$$H = 1 + ar^2 - u^2, \qquad D_g = -1 + ar^2 + u^2, \qquad K = -1 + ar^2 + 3u^2. \tag{3.7}$$

Holding Q fixed while differentiating the mass yields $M_r = H/2$, so $T = H/(4\pi r)$. To obtain the second derivatives, write $4\pi T = r^{-1} + ar - Q^2r^{-3}$. It follows that

$$\begin{aligned} &4\pi(\partial_r T)_Q = -r^{-2} + a + 3Q^2r^{-4} = K/r^2, \\ &M_{SS} = \frac{K}{8\pi^2 r^3}, \qquad M_{SQ} = -\frac{u}{2\pi r^2}, \qquad M_{QQ} = \frac{1}{r}. \end{aligned} \tag{3.8}$$

Here $M_{SQ} = (\partial_Q T)_S$ and $M_{QQ} = (\partial_Q(Q/r))_S$. Taking the determinant subtracts $2u^2$ from K in its numerator. Dividing T by M_{SS} gives the response in the restricted ensemble,

$$\det W = \frac{D_g}{8\pi^2 r^4}, \qquad C_{Q,P} = \frac{2\pi r^2 H}{K}. \tag{3.9}$$

In the notation of Eqs. (5.2) and (5.3), $N(r) = r^2 H$ and $D(r) = r^2 K$. The additional factor D_g vanishes where the two-variable Hessian degenerates.

The coordinates (r, u) diagonalize the metric. Substituting $dS = 2\pi r\, dr$, $dQ = u\, dr + r\, du$ into the quadratic form $W_{SS} dS^2 + 2W_{SQ}\, dS\, dQ + W_{QQ} dQ^2$ gives

$$\begin{aligned} ds_W^2 &= \frac{K}{2r}\, dr^2 - \frac{2u}{r}\, dr\, (u\, dr + r\, du) + \frac{1}{r}(u\, dr + r\, du)^2 \\ &= \frac{D_g}{2r}\, dr^2 + r\, du^2, \qquad ds_g^2 = E\, dr^2 + G\, du^2 = \frac{2\pi}{H}\big(D_g\, dr^2 + 2r^2 du^2\big). \end{aligned} \tag{3.10}$$

On the regular real outer sheet $r > 0$ and $H > 0$. The full metric is positive definite precisely when $D_g > 0$. Its scalar curvature remains well defined on the indefinite patch where $D_g < 0$.

Use $R^i{}_{jkl} = \partial_k \Gamma^i_{lj} - \partial_l \Gamma^i_{kj} + \Gamma^i_{km}\Gamma^m_{lj} - \Gamma^i_{lm}\Gamma^m_{kj}$ and $R_{jl} = R^i{}_{jil}$. For a diagonal metric the distinct connection coefficients, with subscripts after a comma denoting partial derivatives, are

$$\begin{aligned} &\Gamma^r_{rr} = E_{,r}/(2E), && \Gamma^r_{ru} = E_{,u}/(2E), && \Gamma^r_{uu} = -G_{,r}/(2E), \\ &\Gamma^u_{rr} = -E_{,u}/(2G), && \Gamma^u_{ru} = G_{,r}/(2G), && \Gamma^u_{uu} = G_{,u}/(2G). \end{aligned} \tag{3.11}$$

Let $J = EG = 8\pi^2 r^2 D_g/H^2$. Substituting the connection coefficients in $R = 2R_{ruru}/J$ and collecting derivatives of E and G gives

$$R = -\frac{G_{,rr} + E_{,uu}}{J} + \frac{J_{,r}G_{,r} + J_{,u}E_{,u}}{2J^2}. \tag{3.12}$$

The required derivatives follow from the diagonal components,

$$\begin{aligned} G_{,r} &= \frac{8\pi r(1-u^2)}{H^2}, & E_{,u} &= \frac{8\pi a r^2 u}{H^2}, \\ G_{,rr} &= \frac{8\pi(1-u^2)(H - 4ar^2)}{H^3}, & E_{,uu} &= \frac{8\pi a r^2 (H + 4u^2)}{H^3}, \\ \frac{J_{,r}}{J} &= \frac{2}{r} + \frac{2ar}{D_g} - \frac{4ar}{H}, & \frac{J_{,u}}{J} &= \frac{2u}{D_g} + \frac{4u}{H}. \end{aligned} \tag{3.13}$$

Inserting these expressions in Eq. (3.12) yields

$$R = -\frac{a(ar^2 + u^2)(ar^2 + 3u^2 - 3)}{\pi H D_g^2} = \frac{a(D_g + 1)(H - 2D_g)}{\pi H D_g^2}. \tag{3.14}$$

The real scalar in the first form agrees with Eq. (31) of Ref. [19] after restoring the area-entropy normalization $S = \pi r^2$. The second form isolates the leading coefficient at a regular point of $D_g = 0$. For $a > 0$ and $H \neq 0$, it gives

$$D_g^2 R\big|_{D_g = 0} = \frac{a}{\pi}. \tag{3.15}$$

Thus the order is two in a local transverse coordinate D_g. For $a > 0$ at physical extremality $H = 0$ one instead has $u^2 = 1 + ar^2$ and $D_g = 2ar^2 > 0$. Multiplication by H leaves $-2a(D_g + 1)/(\pi D_g) \neq 0$, a simple pole transverse to that boundary. This extremal limit is taken from the patch where $T \neq 0$.

3.3 A flat limit and two distinct pole collisions

At $a = 0$ one has $D_g = -H$ throughout the nonextremal domain $|u| < 1$. Equation (3.10) reduces to

$$ds_g^2 = -2\pi\, dr^2 + \frac{4\pi r^2}{1 - u^2}\, du^2 = -d\rho^2 + \rho^2 d\theta^2, \quad \rho = \sqrt{2\pi}\, r, \quad \theta = \sqrt{2}\arcsin u. \tag{3.16}$$

Setting $X = \rho\cosh\theta$, $Y = \rho\sinh\theta$ gives $ds_g^2 = -dX^2 + dY^2$. This verifies $R = 0$ without taking the limit of Eq. (3.14), in agreement with the RN flatness result [19]. For $Q \neq 0$ the fixed-charge response still has a simple pole at $r^2 = 3Q^2$ since $K = -1 + 3Q^2/r^2$ and $H = 2/3$ there.

For $a > 0$ at fixed $Q \neq 0$, put $x = r^2$. The numerators of K and D_g after multiplication by x are

$$xK = ax^2 - x + 3Q^2, \qquad xD_g = ax^2 - x + Q^2. \tag{3.17}$$

The discriminants are $1 - 12aQ^2$ for the heat-capacity denominator and $1 - 4aQ^2$ for the Hessian determinant. At a simple zero of K, $D_g = -2u^2 \neq 0$. Provided $H \neq 0$, the two-variable curvature is regular at this canonical response pole. The discriminants vanish on different isobars, where we can also compare the orders of the poles.

At $aQ^2 = 1/12$, completing the square gives $K = a(r^2 - r_c^2)^2/r^2$ with $r_c^2 = 1/(2a) = 6Q^2$. At this radius $(H, D_g) = (4/3, -1/3)$. Since $r^2 - r_c^2 = (r - r_c)(2r_c + r - r_c)$, the leading term of K is $4a(r - r_c)^2$. Consequently,

$$\lim_{r\to r_c}(r - r_c)^2 C_{Q,P} = \frac{2\pi r_c^2(4/3)}{4a} = 48\pi Q^4, \qquad R(r_c) = \frac{3}{4\pi Q^2}. \tag{3.18}$$

The double pole belongs to the heat capacity along the fixed-Q slice. At the same state, the curvature of the full (S, Q) metric is finite. Since $D_g = -1/3$, the metric is indefinite and cannot describe a positive quadratic form for simultaneous entropy and charge fluctuations.

At $aQ^2 = 1/4$, the factorization is instead $D_g = a(r^2 - r_*^2)^2/r^2$, where $r_*^2 = 1/(2a) = 2Q^2$. This gives $D_g = 4a(r - r_*)^2 + O((r - r_*)^3)$, while $H = K = 1$ at r_*. Combining Eq. (3.15) with this quadratic contact yields

$$\lim_{r\to r_*}(r - r_*)^4 R = \frac{1}{16\pi a}, \qquad C_{Q,P}(r_*) = 2\pi r_*^2 = 4\pi Q^2. \tag{3.19}$$

The fixed-charge curve touches the degeneracy locus quadratically, so it samples a fourth-order pole even though the transverse pole has order two. More generally, the order along a curve follows by composition. If $R = bD_g^{-2} + O(D_g^{-1})$ and $D_g(t) = c(t - t_*)^m + O((t - t_*)^{m+1})$ with $bc \neq 0$, then $R(t) \sim bc^{-2}(t - t_*)^{-2m}$. A pole order measured along a thermodynamic path thus depends on its order of contact with the degeneracy locus.

3.4 Which response does the curvature pole detect?

Holding the electric potential fixed gives a response governed by the Hessian determinant. To see this for a general two-variable potential at fixed P, write $W = \left(\begin{smallmatrix} A_0 & B_0 \\ B_0 & E_0 \end{smallmatrix}\right)$. Then $dT = A_0 dS + B_0 dQ$ and $d\Phi = B_0 dS + E_0 dQ$. Along a curve of fixed Φ, the second differential gives $dQ = -B_0 dS/E_0$ when $E_0 \neq 0$. Inserting this expression into dT gives

$$\left(\frac{\partial T}{\partial S}\right)_{\Phi,P} = A_0 - \frac{B_0^2}{E_0} = \frac{\det W}{E_0}, \qquad C_{\Phi,P} = \frac{TE_0}{\det W} = \frac{2\pi r^2 H}{D_g} \quad \text{for RN–AdS.} \tag{3.20}$$

The last equality uses $E_0 = 1/r$ and Eq. (3.9). Equivalently, the electric potential is $u = \Phi = Q/r$, giving $4\pi r^2(\partial_r T)_{\Phi,P} = -1 + ar^2 + \Phi^2 = D_g$. Within the same equation of state, $K = 0$ marks a stationary temperature at fixed charge and $D_g = 0$ a stationary temperature at fixed potential [22, 39, 40]. The fixed-charge slices in Fig. 1 specify the path along which we evaluate the curvature of the full two-variable metric.

When $Q = 0$, the mixed derivative vanishes and the two loci coincide. In this limit one can also compare the local instability with the Hawking–Page transition. With $a = 3/\ell^2$, the uncharged temperature $T = (1 + 3r^2/\ell^2)/(4\pi r)$ has its minimum at $r = \ell/\sqrt{3}$. Subtracting TS from the mass gives $G = r(1 - r^2/\ell^2)/4$. With thermal AdS as the zero of G, the Hawking–Page crossing occurs at $r = \ell$ [41]. The two local responses therefore pick out the temperature minimum, while the equality of free energies occurs at a larger radius.

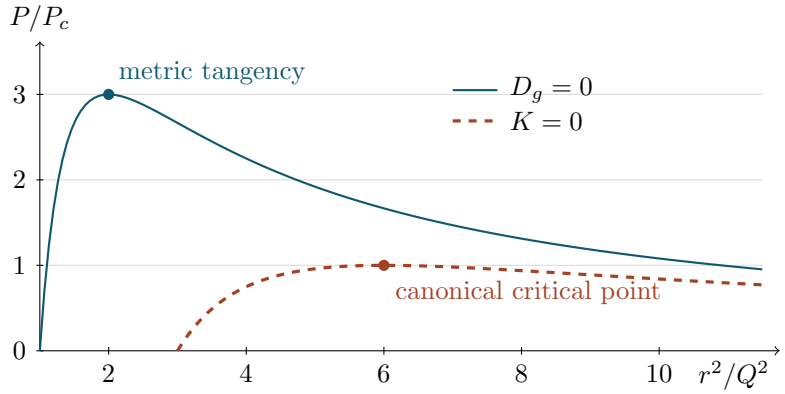

Figure 1: Degeneracy of the two-variable metric (solid) and divergence of the fixed-charge heat capacity (dashed). With $y = r^2/Q^2$ and $p = P/P_c = 12aQ^2$, the curves satisfy $p = 12(y-1)/y^2$ and $p = 12(y-3)/y^2$. A horizontal line at $p = 1$ is tangent to the response locus at $y = 6$. At $p = 3$ it is tangent to the metric-degeneracy locus at $y = 2$.

4 Reconstructing thermodynamic data from a residue field

How much of the two-variable metric can be reconstructed if the optical residue is known throughout a family? Fix P, use the affine mass-representation coordinates (S, Q), and normalize the Killing time in the same way for every state. On a patch with finite, nonzero T, the residue is $b(S, Q) = [4\pi T(S, Q)]^{-1}$. Since $M_S = T$ by the first law, differentiating it gives the entropy row of $g^R_{ij} = M_{ij}/T$,

$$g^R_{SS} = \frac{T_S}{T} = -\partial_S \log b = \frac{1}{C_{Q,P}}, \qquad g^R_{SQ} = \frac{T_Q}{T} = -\partial_Q \log b. \tag{4.1}$$

The derivative ∂_Q in the second component holds S fixed. To recover the mass, integrate $M_S = T$ along each constant-Q curve from the same reference entropy S_0. Differentiating the result twice with respect to charge gives the remaining component,

$$M(S, Q) = \int_{S_0}^{S} \frac{ds}{4\pi b(s, Q)} + F(Q), \qquad g^R_{QQ} = \frac{1}{T}\left[\int_{S_0}^{S} \partial_Q^2 T(s, Q)\, ds + F''(Q)\right]. \tag{4.2}$$

The integration function is the mass $F(Q) = M(S_0, Q)$ on the reference curve. Even complete temperature data on the patch leave its second derivative undetermined. Measuring the electric potential $M_Q(S_0, Q) = F'(Q)$ along the reference curve would supply that charge response. Data confined to a single charge give only the first entry in Eq. (4.1).

Two curvatures for the same temperature field. The missing charge derivative can change a scalar, even when both metrics are positive definite. Consider a family of analytic potentials on a dimensionless affine (S, Q) chart,

$$M_\lambda = \frac{S^3}{6} + SQ + \frac{\lambda Q^2}{2}, \qquad T = \frac{S^2}{2} + Q, \qquad h = M''_\lambda = \begin{pmatrix} S & 1 \\ 1 & \lambda \end{pmatrix}, \qquad \Delta = \det h = \lambda S - 1. \tag{4.3}$$

Varying λ leaves b unchanged and gives the same $C_Q = T/S$ wherever $S \neq 0$. Work on a patch with $\lambda > 0$, $\Delta > 0$ and $T > 0$. Completing the square yields $h_{ij}dx^i dx^j = \lambda(dQ + dS/\lambda)^2 + (S - 1/\lambda)dS^2$. In the coordinates $\sqrt{\lambda}(Q + S/\lambda)$ and $\int^S \sqrt{s - 1/\lambda}\, ds$, this is the Euclidean metric, with $R[h] = 0$. The two-dimensional conformal transformation law in our curvature convention reads $R[h/T] = T(R[h] + \nabla_h^2 \log T)$. The gradient simplifies because $\partial_j T = h_{Sj}$, so $h^{ij}\partial_j \log T = \delta^i_S/T$. Its

divergence gives

$$R[h/T] = \frac{T}{\sqrt{\Delta}}\,\partial_S\left(\frac{\sqrt{\Delta}}{T}\right) = \frac{\partial_S\Delta}{2\Delta} - \frac{\partial_S T}{T} = \frac{\lambda}{2(\lambda S-1)} - \frac{S}{T}. \tag{4.4}$$

At $S = Q = 1$, both choices give $T = 3/2$ and a positive-definite metric. Yet $\lambda = 2$ gives $R = 1/3$ and $\lambda = 3$ gives $R = 1/12$. The example establishes nonuniqueness within analytic thermodynamics. It makes no assumption that a black hole realizes either potential.

A converse on a fixed-control curve. Now suppose that the available data are the entropy and heat capacity along a connected complex state curve of dimension one. Form the measured one-form $\eta = dS/C_{Q,P}$. Any compatible temperature must satisfy $\eta = dT/T = -db/b$ wherever T is finite and nonzero. On a disk where η is holomorphic, one temperature measurement $T(z_0) \neq 0$ fixes the integration constant,

$$T(z) = T(z_0)\exp\left(\int_{z_0}^{z}\eta\right). \tag{4.5}$$

Assume η is holomorphic away from a discrete set of punctures. Two conditions determine whether Eq. (4.5) gives a single-valued meromorphic temperature on the whole curve. On the punctured curve every closed path must satisfy $\oint_\gamma \eta \in 2\pi i\mathbb{Z}$. This condition is also sufficient for single-valuedness there, because changing the integration path multiplies T by the exponential of the added period.

At each puncture, η must in addition have at most a simple pole. To see necessity, write a nonzero meromorphic temperature germ as $T = u^n v(u)$ in a local coordinate u, with $n \in \mathbb{Z}$ and v holomorphic and nonvanishing at 0. Then $\eta = n\,du/u + dv/v$. For sufficiency, write $\eta = (n/u + k(u))du$ with k holomorphic. The period condition around a small circle forces $n \in \mathbb{Z}$, and $u^n \exp(\int k\,du)$ extends the temperature across the puncture up to the fixed normalization. A pole of order $p \geq 2$ in η contributes a nonconstant polynomial in u^{-1} to its primitive. Exponentiation then gives an essential singularity whenever the monodromy is trivial. These conditions determine what can be reconstructed along the chosen curve. The function $F(Q)$ in Eq. (4.2) still requires transverse data.

5 Canonical response on a complexified RN–AdS isobar

Consider a four-dimensional spherical Reissner–Nordström–AdS black hole with real fixed $Q \neq 0$ and $P = -\Lambda/(8\pi) > 0$. We use $G = \hbar = c = k_{\mathrm{B}} = 1$. Here z is the complexified *outer-horizon radius as a state parameter*. Varying it along the isobar changes the mass from one equilibrium solution to the next. In the spacetime calculation the radial coordinate varies within a single metric of fixed mass. The stability analysis of the fixed-charge AdS ensemble follows Refs. [40, 42]. We interpret the cosmological constant as a pressure and the mass as enthalpy in the first law [43–45].

5.1 From the fundamental relation to a meromorphic response

Solving the real horizon condition $f(r) = 1 - 2M/r + Q^2/r^2 + 8\pi P r^2/3 = 0$ for the enthalpy M and continuing the resulting expression and area entropy to complex z gives

$$M(z) = \frac{z}{2} + \frac{Q^2}{2z} + \frac{4\pi P}{3}z^3, \qquad S(z) = \pi z^2. \tag{5.1}$$

Dividing $M'(z) = 1/2 - Q^2/(2z^2) + 4\pi P z^2$ by $S'(z) = 2\pi z$ gives

$$T(z) = \frac{1}{4\pi}\left(8\pi P z + \frac{1}{z} - \frac{Q^2}{z^3}\right) = \frac{N(z)}{4\pi z^3}, \qquad N(z) = 8\pi P z^4 + z^2 - Q^2, \tag{5.2}$$

$$T'(z) = \frac{1}{4\pi}\left(8\pi P - \frac{1}{z^2} + \frac{3Q^2}{z^4}\right) = \frac{D(z)}{4\pi z^4}, \qquad D(z) = 8\pi P z^4 - z^2 + 3Q^2. \tag{5.3}$$

Holding M fixed while differentiating the lapse with respect to the spacetime radius w gives $f_w = 2M/w^2 - 2Q^2/w^3 + 16\pi P w/3$. Only after differentiating set $w = z$ and $M = M(z)$ from Eq. (5.1). This yields $f_w(z; M(z)) = N(z)/z^3 = 4\pi T(z)$. The optical residue and its solution-family derivative are therefore

$$b(z) = \frac{z^3}{N(z)}, \qquad b'(z) = \frac{z^2[3N(z) - zN'(z)]}{N(z)^2} = -\frac{z^2 D(z)}{N(z)^2}. \tag{5.4}$$

Thus the spinodal is directly visible as a stationary optical residue where $T \neq 0$. Independently, differentiation of the enthalpy at fixed S yields $\Phi = Q/z$ and $V = 4\pi z^3/3$, so $dM = T\,dS + \Phi\,dQ + V\,dP$.

These expressions are holomorphic on the punctured z-plane. Where temperature is a local coordinate, the chain rule gives the heat capacity

$$C_{P,Q} = T\left(\frac{\partial S}{\partial T}\right)_{P,Q} = \frac{T(z)\,2\pi z}{T'(z)} = 2\pi z^2\,\frac{N(z)}{D(z)}. \tag{5.5}$$

The rational expression extends the heat capacity meromorphically. On the outer branch, $r > 0$ and $T(r) > 0$, so D determines the sign of $C_{P,Q}$. At a positive zero of D, substituting $3Q^2 = r^2 - 8\pi P r^4$ gives $N = (32\pi P r^4 + 2r^2)/3 > 0$. Each such zero therefore gives a genuine heat-capacity pole. Its effect on a contour integral depends on the differential. Multiplying by $dT = T'(z)\,dz$ gives

$$C_{P,Q}\,dT = T\,dS = M'(z)\,dz. \tag{5.6}$$

The right-hand side is regular across each nonzero spinodal. A small contour around it therefore gives zero for the integral of $C_{P,Q}\,dT$.

5.2 Spinodal multiplicity and ramification of the inverse map

Put $y = r^2$ in $D = 0$. The positive roots can merge only when the discriminant $1 - 96\pi P Q^2$ of $8\pi P y^2 - y + 3Q^2$ vanishes. The quadratic formula and substitution into (5.2) yield

$$y_\pm = \frac{1 \pm \sqrt{1 - 96\pi P Q^2}}{16\pi P}, \qquad P_c = \frac{1}{96\pi Q^2}, \quad r_c^2 = 6Q^2, \quad T_c = \frac{1}{3\pi r_c}. \tag{5.7}$$

These critical values agree with Ref. [45], Eqs. (3.16)–(3.18). The merger of the Davies radii also produces fractional powers in the free energy, as found in Ref. [46]. Below criticality, $0 < P < P_c$, both roots are positive and give simple zeros of T'. The quadratic D opens upward in r^2, so $C_{P,Q} < 0$ between the two spinodal radii. At $P > P_c$ the roots leave the real axis and $C_{P,Q} > 0$ along the physical outer branch. At $P = P_c$ the spinodals merge, giving $D = 8\pi P_c (r^2 - r_c^2)^2$. Differentiating (5.3) twice identifies the first nonzero temperature derivative at the merger,

$$T'' = \frac{2z^{-3} - 12Q^2 z^{-5}}{4\pi}, \qquad T''' = \frac{-6z^{-4} + 60Q^2 z^{-6}}{4\pi}, \qquad T'''(r_c) = \frac{1}{\pi r_c^4}. \tag{5.8}$$

The order of the zero determines the local form of the inverse temperature map. Write $\delta = z - z_0$ and suppose $T'(z) = \alpha\delta^m + O(\delta^{m+1})$, $\alpha \neq 0$, and $T_0 S_0' \neq 0$, with $T_0 = T(z_0)$ and $S_0' = S'(z_0)$. Integrating the expansion of T' and dividing TS' by the same expansion gives

$$T - T_0 = \frac{\alpha}{m+1}\delta^{m+1}\,[1 + O(\delta)], \qquad C_{P,Q} = \frac{T_0 S_0'}{\alpha}\,\delta^{-m}[1 + O(\delta)]. \tag{5.9}$$

The analytic factor multiplying δ^{m+1} is nonzero at the origin of the local coordinate and hence has a holomorphic $(m+1)$st root on a sufficiently small disk. After absorbing this root into the local coordinate, $T - T_0$ is exactly its $(m+1)$st power. On each inverse sheet this gives

$$C_{P,Q}(T) \;\propto\; (T - T_0)^{-m/(m+1)}. \tag{5.10}$$

An ordinary spinodal ($m = 1$) gives a square-root branch point of the inverse, whereas the critical point ($m = 2$) gives a cube-root branch point. Along the critical isobar at fixed P, Q, the heat capacity therefore diverges with exponent $2/3$ as a function of temperature. A locally biholomorphic change of state parameter preserves m because its Jacobian multiplies the temperature derivative by a nonzero analytic factor. At a turning point, using temperature itself as the coordinate loses this invertibility.

Figure 2 shows how an observer following the real isobar encounters the same stationary states in two reciprocal functions. The heat-capacity sign follows from their slopes and the positive entropy slope.

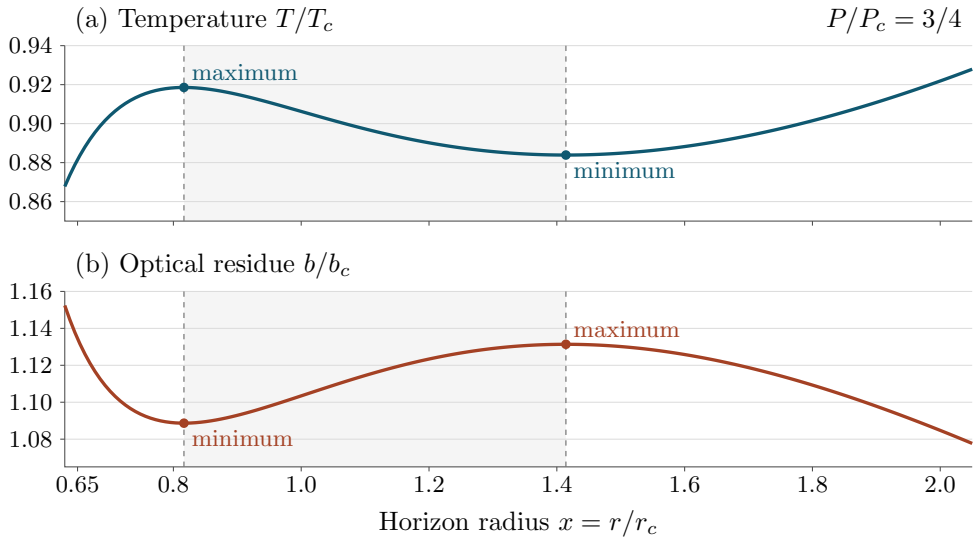

Figure 2: Dimensionless temperature and optical residue on the isobar $p = 3/4$. The dashed guides mark $x_- = \sqrt{2/3}$ and $x_+ = \sqrt{2}$. Temperature reaches a maximum and a minimum, respectively, while the reciprocal $b/b_c = T_c/T$ reverses both extrema. The shaded interval has $C_{P,Q} < 0$. The window $0.63 \le x \le 2.05$ lies on the positive-temperature side of extremality at $x_e \simeq 0.39671$.

5.3 A contour count with a real-slice check

Let $x = z/r_c$, $p = P/P_c$, and $\tau = T/T_c$. Substitution of (5.7) into (5.2) gives

$$\tau_p(x) = \frac{3px + 6x^{-1} - x^{-3}}{8}, \qquad \chi_p(x) = \frac{d\tau_p}{dx} = \frac{3}{8x^4}\big(px^4 - 2x^2 + 1\big). \tag{5.11}$$

The quartic in Eq. (5.11) also appears in the spinodal analysis of Xu and Mann [34, Eq. (8)]. Its zeros enter the logarithmic derivative of the temperature slope with their multiplicities. For a positively oriented simple contour Γ avoiding the zeros and poles of χ_p, the argument principle [47, Chap. 3] gives

$$W_\Gamma = \frac{1}{2\pi i}\oint_\Gamma \frac{\chi_p'(x)}{\chi_p(x)}\,dx = \sum_{\text{inside } \Gamma} \operatorname{ord}_x(\chi_p). \tag{5.12}$$

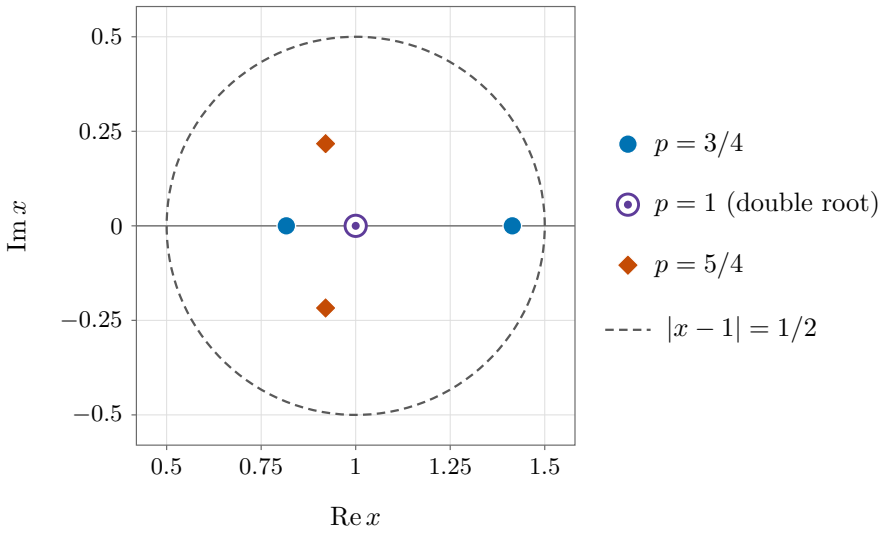

Figure 3: Zeros of the reduced temperature derivative $\chi_p = d(T/T_c)/dx$ in the disk $|x-1| < 1/2$, where $x = z/r_c$ and $p = P/P_c$. Two real zeros at $p = 3/4$ coalesce at $p = 1$ and form a complex-conjugate pair at $p = 5/4$. The winding on the dashed contour is two in all three cases.

To see the local contribution, write $\chi_p = (x - x_j)^{k_j} h_j(x)$ with $h_j(x_j) \neq 0$. Then $\chi_p'/\chi_p = k_j/(x - x_j) + h_j'/h_j$, with residue k_j. The fourth-order pole at $x = 0$ carries index -4 and lies outside the circle $|x - 1| = 1/2$. The four roots satisfy $x^2 = (1 \pm \sqrt{1-p})/p$. The table lists those inside the circle for three isobars.

p	Enclosed roots	W_Γ	Distinct real enclosed roots
$3/4$	$\sqrt{2/3},\ \sqrt{2}$	2	2
1	1 (multiplicity two)	2	1
$5/4$	$\sqrt{(4+2i)/5},\ \sqrt{(4-2i)/5}$	2	0

The conjugate roots in the last row, approximately $0.9204 \pm 0.2173i$, both lie within $1/2$ of 1. The partners with negative real part lie outside the disk for all three isobars. As the zeros move off the real axis, the contour retains their total multiplicity. Only the positive-temperature roots on the real axis correspond to physical spinodals.

Figure 3 locates the zeros and the integration contour explicitly.

For a numerical check, set $w_k = R\exp(2\pi ik/n)$ and $x_k = c + w_k$ on a circle of centre c and radius R. Substitution into (5.12) gives the trapezoidal estimate $n^{-1}\sum_{k=0}^{n-1} w_k\, \tau_p''(x_k)/\tau_p'(x_k)$. With 60 decimal digits and $n = 256$, numerical differentiation of τ_p reproduced all three exact counts to absolute error below 1.2×10^{-21}. At $p = 3/4$, a circle of radius $1/12$ around either positive root gave index 1. A circle of radius $1/4$ about 0 at $p = 5/4$ gave -4, the index of the fourth-order pole.

5.4 Coexistence from two radii

Coexistence requires two stable equilibria at the same P, Q, T to have equal Gibbs free energy. The relevant potential follows from (5.1) and (5.2),

$$G(r) = M(r) - T(r)S(r) = \frac{r}{4} + \frac{3Q^2}{4r} - \frac{2\pi P}{3}r^3, \qquad dG = -S\,dT \quad (P, Q \text{ fixed}). \tag{5.13}$$

Let $a < b$ be the two competing radii, and set $v = ab$, $s = a+b$, $h = a^2+ab+b^2$. Divide the equal-temperature condition $T(a) - T(b) = 0$ and the equal-free-energy condition $4[G(a) - G(b)] = 0$ by $a - b$. With $(a^{-1} - b^{-1})/(a - b) = -1/v$ and $(a^{-3} - b^{-3})/(a - b) = -h/v^3$, the two conditions become

$$8\pi P = \frac{1}{v} - \frac{Q^2 h}{v^3}, \qquad \frac{8\pi P}{3}h = 1 - \frac{3Q^2}{v}. \tag{5.14}$$

Eliminating P and multiplying by v^3 gives $(h-3v)[v^2-Q^2(h+3v)]=0$. Here $h-3v=(a-b)^2>0$. Since $h+3v=s^2+2v$,

$$Q^2=\frac{v^2}{s^2+2v},\qquad 8\pi P=\frac{3Q^2}{v^2},\qquad v=\frac{6Q^2}{\sqrt{p}},\qquad s^2=\frac{v^2}{Q^2}-2v. \tag{5.15}$$

Taking $s>0$, the two solutions of $r^2-sr+v=0$ are real, positive and distinct when $s^2-4v=v(v/Q^2-6)>0$, i.e., $0<p<1$. Inserting these relations into $D(r)$ gives

$$D(r)=\frac{2r^2(a-b)^2}{s^2+2v}>0\qquad (r=a,b). \tag{5.16}$$

At the common temperature found below, both coexistence radii have finite positive heat capacity. The off-shell potential at bath temperature T_* is $M(r)-T_*S(r)$. Its first derivative is $(T(r)-T_*)S'(r)$, and at a stationary radius its second derivative is $T'(r)S'(r)$. The two positive-slope branches are local minima. Any intervening negative-slope branch is a local maximum; Eq. (5.3) permits at most three positive-temperature stationary radii at fixed bath temperature. The comparison is within the spherical charged family. At either radius the equality $4\pi T=8\pi Pr+1/r-Q^2/r^3$ reduces to $T_*=Q^2s/(\pi v^2)$. For example, at $r=a$, multiplication by v^3/Q^2 gives $3av+b(s^2+2v)-b^3=4vs$. Squaring T_*/T_c, substituting $r_c^2=6Q^2$ and expressing s,v in terms of the reduced pressure gives

$$\left(\frac{T_*}{T_c}\right)^2=\frac{54Q^6s^2}{v^4}=\frac{54Q^4}{v^2}\left(1-\frac{2Q^2}{v}\right)=\frac{p}{2}(3-\sqrt{p}). \tag{5.17}$$

Maxwell's equal-area construction gives the same coexistence curve in Ref. [48], Eq. (23). Equation (5.16) explains why a search for poles on either branch misses this transition. The Gibbs free energies cross while both heat capacities are finite.

5.5 Comparison with the normalized temperature–volume curvature

The canonical spinodal appears as a curvature singularity in the normalized temperature–volume geometry. In the (T,V) construction of Wei, Liu and Mann [49], the volume is $V=4\pi r^3/3$. Since $S=\pi r^2$ is fixed when V is fixed, $C_V=0$. Their prescription treats C_V as a small constant in the metric and retains the normalized quantity $R_N=C_VR_{(T,V)}$ in their curvature convention. This limiting prescription distinguishes the normalized quantity from the ordinary scalar in Eq. (3.14). Recent work relates its divergence to folds of the temperature curve [50].

To compare the curvatures along the same isobar, write $x=r/r_c$, $\tau=T/T_c$, and $v=V/V_c=x^3$. Define $L=3x^2-1$ and $B_*=2\tau x^3$. Equation (13) of Ref. [49] takes the form

$$R_N=\frac{L(L-2B_*)}{2(L-B_*)^2}=\frac{1}{2}\left[1-\left(\frac{B_*}{L-B_*}\right)^2\right], \tag{5.18}$$

where the second expression follows by completing the square in the numerator. On the isobar, Eq. (5.11) gives $L-B_*=-3(px^4-2x^2+1)/4=-2x^4\tau_p'(x)$. Dividing by this expression gives $B_*/(L-B_*)=-\tau/(x\tau_p')$. The entropy derivative $dS/dx=2S/x$ gives $C_{P,Q}=2S\tau/(x\tau_p')$. On every regular branch, substitution into the square gives the meromorphic identity

$$R_N=\frac{1}{2}\left[1-\left(\frac{C_{P,Q}}{2S}\right)^2\right]. \tag{5.19}$$

At a simple canonical spinodal with $S\neq 0$, squaring the heat capacity gives R_N a double pole in r. At $p=1$, Eq. (3.18) gives $C_{P,Q}/(2S)\sim 4Q^2/(r-r_c)^2$, and hence $R_N\sim -8Q^4/(r-r_c)^4$. At the $p=3$ tangency, $C_{P,Q}=2S$ and $R_N=0$, while the ordinary fixed-pressure scalar has a fourth-order pole. The different values persist even with the state and the direction of approach held fixed, because the two constructions use different metrics and the temperature–volume curvature includes a regulator.

Figure 4 compares the two limiting isobars using the same underlying state functions.

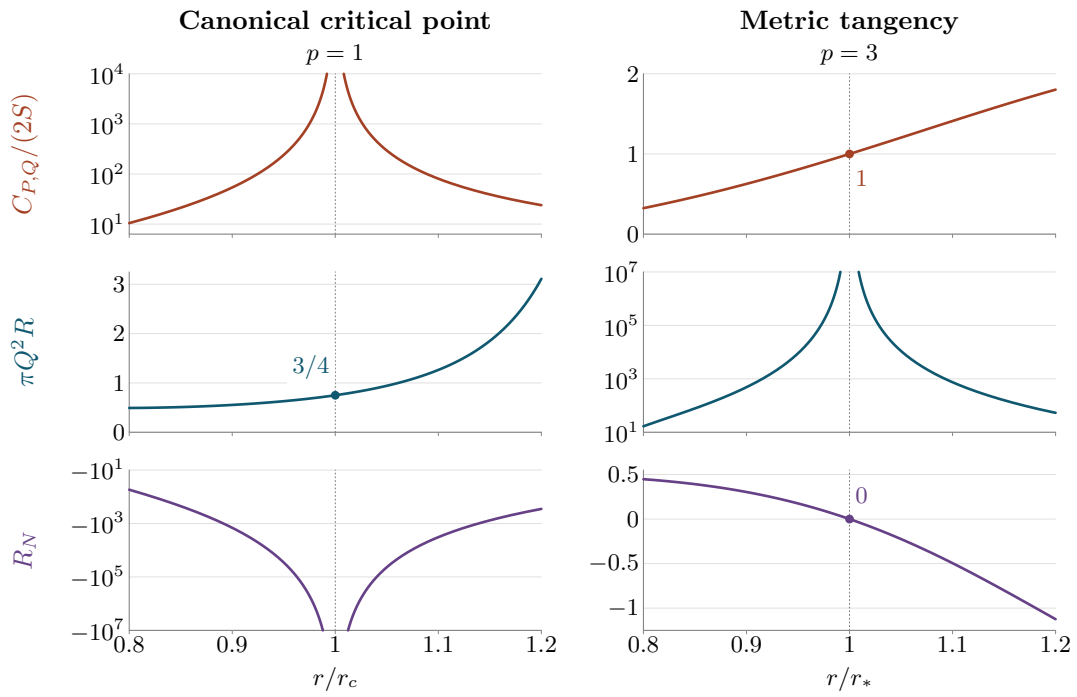

Figure 4: Fixed-charge isobars through the canonical critical point (left, $r_c^2 = 6Q^2$) and the tangency to the metric-degeneracy locus (right, $r_*^2 = 2Q^2$). Rows show the heat-capacity ratio, the ordinary (S, Q) curvature, and the normalized (T, V) curvature of Eq. (5.19). The divergent panels use logarithmic spacing in magnitude, with the sign retained on the tick labels. The three finite panels use linear scales. Dotted lines mark the central radii. Dots give the regular values there. Curves end at the frame when their magnitude exceeds the displayed range.

6 Discussion and conclusions

A temperature field gives access to two entries of the fixed-pressure entropy metric. With $b = (4\pi T)^{-1}$, its entropy row is the gradient of $-\log b$ in (S, Q). Integration in S leaves a function $F(Q)$ whose second derivative enters the remaining diagonal entry. The missing function can be obtained from electrical data. Specifying the electric potential $\Phi(S_0, Q)$ along one reference curve fixes $F'(Q)$. A well-defined optical pole alone supplies even less information when the spacetime has unconventional asymptotics and the conserved mass has yet to be identified [13].

For RN–AdS one can locate the two singularity loci using real derivatives of the equation of state. The fixed-charge slope gives $K = 4\pi r^2(\partial_r T)_{Q,P}$, and the fixed-potential slope gives $D_g = 4\pi r^2(\partial_r T)_{\Phi,P}$. At a regular zero of D_g, $D_g^2 R \to 8P$. A curve with quadratic contact there records a fourth-order pole in its radius parameter. This is one reason to specify both the metric and the approach to the singular state. An (S, Φ) construction with a partially transformed potential [51], a canonical free-energy metric [52], and the normalized curvature R_N in (T, V) [49, 50] refer to different fluctuation problems. According to Eq. (5.19), R_N diverges at the canonical critical point where the ordinary (S, Q) scalar equals $3/(4\pi Q^2)$.

The interpretation of a winding number likewise depends on the function traced around the contour. The zeros of the temperature derivative count stationary points with multiplicity. Zeros of the difference between the Hawking and bath temperatures count equilibrium states at a specified bath temperature [30]. The real signed index of a zero of inverse heat capacity is a third construction [53]. Lee–Yang zeros instead require a statistical partition function [54]. In the present family the contour index stays at two as the spinodal roots move off the real axis. The coexistence temperature requires the values of the free energy at two distinct real radii. These two calculations use the same equation of state and answer different physical questions.

References

[1] J. M. Bardeen, B. Carter, and S. W. Hawking, The four laws of black hole mechanics. *Communications in Mathematical Physics* **31**, 161–170 (1973). 10.1007/BF01645742.

[2] Jacob D. Bekenstein, Black holes and entropy. *Physical Review D* **7**, 2333–2346 (1973). 10.1103/PhysRevD.7.2333.

[3] S. W. Hawking, Particle creation by black holes. *Communications in Mathematical Physics* **43**, 199–220 (1975). 10.1007/BF02345020.

[4] J. B. Hartle and S. W. Hawking, Path-integral derivation of black-hole radiance. *Physical Review D* **13**, 2188–2203 (1976). 10.1103/PhysRevD.13.2188.

[5] G. W. Gibbons and S. W. Hawking, Action integrals and partition functions in quantum gravity. *Physical Review D* **15**, 2752–2756 (1977). 10.1103/PhysRevD.15.2752.

[6] K. Srinivasan and T. Padmanabhan, Particle production and complex path analysis. *Physical Review D* **60**, 024007 (1999). 10.1103/PhysRevD.60.024007.

[7] Maulik K. Parikh and Frank Wilczek, Hawking radiation as tunneling. *Physical Review Letters* **85**, 5042–5045 (2000). 10.1103/PhysRevLett.85.5042.

[8] L. Vanzo, G. Acquaviva, and R. Di Criscienzo, Tunnelling methods and Hawking's radiation: achievements and prospects. *Classical and Quantum Gravity* **28**, 183001 (2011). 10.1088/0264-9381/28/18/183001.

[9] Charles W. Robson, Leone Di Mauro Villari, and Fabio Biancalana, Topological nature of the Hawking temperature of black holes. *Physical Review D* **99**, 044042 (2019). 10.1103/PhysRevD.99.044042.

[10] Sang Pyo Kim, Hawking radiation as quantum tunneling in Rindler coordinate. *J. High Energy Phys.* **11**, 048 (2007). 10.1088/1126-6708/2007/11/048.

[11] Wen-Xiang Chen and Yao-Guang Zheng, Calculating the Hawking temperatures of Kerr–Newman black holes in the f(R) gravity models with the RVB method. *International Journal of Modern Physics A* **40**, 2550077 (2025). 10.1142/S0217751X25500770.

[12] Wen-Xiang Chen, Calculating the Hawking temperature of black holes in f(Q) gravity using the RVB method: a residue-based approach. *Canadian Journal of Physics* **103**, 531–542 (2025). 10.1139/cjp-2024-0214.

[13] Wen-Xiang Chen, Horizon residues and test-scalar quasinormal modes of a perturbative Schwarzschild-type black hole in quadratic f(Q) gravity. *European Physical Journal C* **86**, 991 (2026). 10.1140/epjc/s10052-026-16260-4.

[14] Wen-Xiang Chen, *Higher-Dimensional Black Hole Hawking Temperature and Entropy from the RVB–Residue Method: Tangherlini–AdS and Einstein–Gauss–Bonnet Examples*. Cambridge Open Engage, working paper, version 1 (2026). 10.33774/coe-2026-48jjt.

[15] Wen-Xiang Chen, *Geometry as Thermodynamics: Entropy Stationarity and Horizon Residues*. arXiv:2609.30660 [gr-qc], preprint (2026). Record.

[16] F. Weinhold, Metric geometry of equilibrium thermodynamics. *J. Chem. Phys.* **63**, 2479–2483 (1975). 10.1063/1.431689.

[17] G. Ruppeiner, Thermodynamics: A Riemannian geometric model. *Phys. Rev. A* **20**, 1608–1613 (1979). 10.1103/PhysRevA.20.1608.

[18] G. Ruppeiner, Riemannian geometry in thermodynamic fluctuation theory. *Rev. Mod. Phys.* **67**, 605–659 (1995). Erratum, Rev. Mod. Phys. 68, 313 (1996). 10.1103/RevModPhys.67.605.

[19] J. E. Åman, I. Bengtsson, and N. Pidokrajt, Geometry of black hole thermodynamics. *Gen. Relativ. Gravit.* **35**, 1733–1743 (2003). 10.1023/A:1026058111582.

[20] P. C. W. Davies, The thermodynamic theory of black holes. *Proc. R. Soc. Lond. A* **353**, 499–521 (1977). 10.1098/rspa.1977.0047.

[21] J. Shen, R.-G. Cai, B. Wang, and R.-K. Su, Thermodynamic geometry and critical behavior of black holes. *Int. J. Mod. Phys. A* **22**, 11–27 (2007). 10.1142/S0217751X07034064.

[22] H. Liu, H. Lü, M. Luo, and K.-N. Shao, Thermodynamical metrics and black hole phase transitions. *J. High Energy Phys.* **12**, 054 (2010). 10.1007/JHEP12(2010)054.

[23] S. A. Hosseini Mansoori, B. Mirza, and M. Fazel, Hessian matrix, specific heats, Nambu brackets, and thermodynamic geometry. *J. High Energy Phys.* **04**, 115 (2015). 10.1007/JHEP04(2015)115.

[24] B. Mirza and M. Zamani-Nasab, Ruppeiner geometry of RN black holes: flat or curved? *J. High Energy Phys.* **06**, 059 (2007). 10.1088/1126-6708/2007/06/059.

[25] G. Ruppeiner, Thermodynamic curvature and phase transitions in Kerr–Newman black holes. *Phys. Rev. D* **78**, 024016 (2008). 10.1103/PhysRevD.78.024016.

[26] H. Quevedo, Geometrothermodynamics. *J. Math. Phys.* **48**, 013506 (2007). 10.1063/1.2409524.

[27] Wen-Xiang Chen and Yao-Guang Zheng, Thermodynamic geometric analysis of RN black holes under f(R) gravity. *Canadian Journal of Physics* **104**, 1–27 (2026). 10.1139/cjp-2025-0237.

[28] Shao-Wen Wei, Yu-Xiao Liu, and Robert B. Mann, Black hole solutions as topological thermodynamic defects. *Phys. Rev. Lett.* **129**, 191101 (2022). 10.1103/PhysRevLett.129.191101.

[29] Chaoxi Fang, Jie Jiang, and Ming Zhang, Revisiting thermodynamic topologies of black holes. *J. High Energy Phys.* **01**, 102 (2023). 10.1007/JHEP01(2023)102.

[30] Zhen-Ming Xu, Yu-Shan Wang, Bin Wu, and Wen-Li Yang, Generalized Maxwell equal area law and black holes in complex free energy. *Phys. Lett. B* **850**, 138528 (2024). 10.1016/j.physletb.2024.138528.

[31] Yu-Shan Wang, Zhen-Ming Xu, and Bin Wu, Thermodynamic phase transition and winding number for the third-order Lovelock black hole. *Chin. Phys. C* **48**, 095101 (2024). 10.1088/1674-1137/ad53ba.

[32] F. Barzi, H. El Moumni, and K. Masmar, Riemann surfaces and winding numbers of Rényi phase structure of charged-flat black holes. *Eur. Phys. J. C* **84**, 1141 (2024). 10.1140/epjc/s10052-024-13511-0.

[33] Shi-Hao Zhang, Shao-Wen Wei, Jing-Fei Zhang, and Xin Zhang, Unifying topological, geometric, and complex classifications of black hole thermodynamics. *Phys. Lett. B* **880**, 140822 (2026). 10.1016/j.physletb.2026.140822.

[34] Zhen-Ming Xu and Robert B. Mann, Thermodynamic supercriticality and complex phase diagram for the AdS black hole. *Phys. Rev. Lett.* **136**, 041402 (2026). 10.1103/c39y-zcz6.

[35] Robert M. Wald, Black hole entropy is the Noether charge. *Physical Review D* **48**, R3427–R3431 (1993). 10.1103/PhysRevD.48.R3427.

[36] Vivek Iyer and Robert M. Wald, Some properties of the Noether charge and a proposal for dynamical black hole entropy. *Physical Review D* **50**, 846–864 (1994). 10.1103/PhysRevD.50.846.

[37] James W. York, Jr., Black-hole thermodynamics and the Euclidean Einstein action. *Physical Review D* **33**, 2092–2099 (1986). 10.1103/PhysRevD.33.2092.

[38] G. W. Gibbons and R. E. Kallosh, Topology, entropy, and Witten index of dilaton black holes. *Physical Review D* **51**, 2839–2862 (1995). 10.1103/PhysRevD.51.2839.

[39] Jorma Louko and Stephen N. Winters-Hilt, Hamiltonian thermodynamics of the Reissner–Nordström–anti-de Sitter black hole. *Phys. Rev. D* **54**, 2647–2663 (1996). 10.1103/PhysRevD.54.2647.

[40] Andrew Chamblin, Roberto Emparan, Clifford V. Johnson, and Robert C. Myers, Holography, thermodynamics, and fluctuations of charged AdS black holes. *Phys. Rev. D* **60**, 104026 (1999). 10.1103/PhysRevD.60.104026.

[41] S. W. Hawking and Don N. Page, Thermodynamics of black holes in anti-de Sitter space. *Commun. Math. Phys.* **87**, 577–588 (1983). 10.1007/BF01208266.

[42] Andrew Chamblin, Roberto Emparan, Clifford V. Johnson, and Robert C. Myers, Charged AdS black holes and catastrophic holography. *Phys. Rev. D* **60**, 064018 (1999). 10.1103/PhysRevD.60.064018.

[43] David Kastor, Sourya Ray, and Jennie Traschen, Enthalpy and the mechanics of AdS black holes. *Class. Quantum Grav.* **26**, 195011 (2009). 10.1088/0264-9381/26/19/195011.

[44] Brian P. Dolan, Pressure and volume in the first law of black hole thermodynamics. *Class. Quantum Grav.* **28**, 235017 (2011). 10.1088/0264-9381/28/23/235017.

[45] David Kubizňák and Robert B. Mann, *P–V* criticality of charged AdS black holes. *J. High Energy Phys.* **07**, 033 (2012). 10.1007/JHEP07(2012)033.

[46] Li-Hua Wang, Yun He, and Meng-Sen Ma, Fractional phase transitions of RN-AdS black holes at their Davies points. *Chinese Physics C* **47**, 035102 (2023). 10.1088/1674-1137/aca957.

[47] Elias M. Stein and Rami Shakarchi, *Complex Analysis*. Princeton Lectures in Analysis, Vol. II, Princeton University Press (2003). ISBN 9780691113852.

[48] Shan-Quan Lan, Jie-Xiong Mo, and Wen-Biao Liu, A note on Maxwell's equal area law for black hole phase transition. *Eur. Phys. J. C* **75**, 419 (2015). 10.1140/epjc/s10052-015-3641-0.

[49] S.-W. Wei, Y.-X. Liu, and R. B. Mann, Repulsive interactions and universal properties of charged anti–de Sitter black hole microstructures. *Phys. Rev. Lett.* **123**, 071103 (2019). 10.1103/PhysRevLett.123.071103.

[50] S.-H. Zhang, J.-F. Zhang, and X. Zhang, *Thermodynamic geometry as the missing link: toward a unified framework for black hole first-order phase transitions*. arXiv:2609.31144 [gr-qc], preprint (2026). Record.

[51] C. Niu, Y. Tian, and X.-N. Wu, Critical phenomena and thermodynamic geometry of Reissner–Nordström–anti-de Sitter black holes. *Phys. Rev. D* **85**, 024017 (2012). 10.1103/PhysRevD.85.024017.

[52] P. Chaturvedi, S. Mondal, and G. Sengupta, Thermodynamic geometry of black holes in the canonical ensemble. *Phys. Rev. D* **98**, 086016 (2018). 10.1103/PhysRevD.98.086016.

[53] Shan-Ping Wu, Si-Jiang Yang, and Shao-Wen Wei, Extended thermodynamical topology of black hole. *European Physical Journal C* **85**, 1372 (2025). 10.1140/epjc/s10052-025-15098-6.

[54] T. D. Lee and C. N. Yang, Statistical theory of equations of state and phase transitions. II. Lattice gas and Ising model. *Phys. Rev.* **87**, 410–419 (1952). 10.1103/PhysRev.87.410.